RSC Advances

ROYAL SOCIETY OF CHEMISTRY

www.rsc.org/advances

Effect of the Blocked-Sites Phenomenon on the Heterogeneous Reaction of Pyrene with $N_2O_5/NO_3/NO_2$

Peng Zhang[†*], *Wanqi Sun*[†], *Bo Yang*[†], *Jinian Shu*[†], *and Liang Dong*[‡]

[†]State Key Joint Laboratory of Environment Simulation and Pollution Control, Research Center for Eco-Environmental Sciences, Chinese Academy of Sciences, Beijing 100085, China

[‡]National Research Center for Environmental Analysis and Measurement, Beijing 100029, China

Abstract

To clarify whether the blocking reaction sites problem has a significant impact on heterogeneous reactions, experiments contrasting the order of pyrene (PY) particles' exposure to $N_2O_5-O_3$ or $O_3-N_2O_5$ in a heterogeneous process were conducted. Additionally, PY particles were exposed to N_2O_5 (~8 ppm) in the presence of O_3 (2.5–30 ppm) in a reaction chamber at ambient pressure and room temperature. Our results show that the phenomenon of blocking reaction sites may be ubiquitous on the surfaces of atmospheric aerosol particles, and the N_2O_5-initiated ionic electrophilic nitration may be promoted by NO_3 radical-initiated heterogeneous

[*] Corresponding author. Tel.: +86 010 62849087; Fax: +86 010 6292 3563.

E-mail address: pengzhang@rcees.ac.cn

[†]Research Center for Eco-Environmental Sciences, Chinese Academy of Sciences

[‡]National Research Center for Environmental Analysis and Measurement, Beijing, China

reactions on the aerosol particle surface. We also found that the operative reaction mechanism strongly depends on the concentrations of the nitric oxides in the atmosphere. Our results provide an explanation as to why 2-nitropyrene (2-NPY), one of the most ubiquitous nitro-polyaromatic hydrocarbon pollutants that exists in both the gas and particle phases, was not observed in previous experiments on the heterogeneous reactions of PY and $N_2O_5/NO_3/NO_2$.

Keywords: Polycyclic aromatic hydrocarbon; Heterogeneous reaction; NO_3 radical; Aerosol mass spectrometry

Introduction

Polycyclic aromatic hydrocarbons (PAHs) are ubiquitous air pollutants resulting from incomplete combustion processes, such as those of diesel and gasoline engines, and biomass or coal burning,[1] and constitute a health risk to the population due to their mutagenic and carcinogenic properties.[2] Homogeneous and heterogeneous processes, promoted by the interaction of PAHs with atmospheric trace oxidants during their atmospheric transit, are considered important degradation pathways for both gas-phase and particulate PAHs. In particular, the heterogeneous chemistry between particulate PAHs and gas-phase oxidants has been shown to be one of the most important sources of the more toxic and mutagenic PAH derivatives (nitro-PAHs (NPAHs) and oxy-PAHs).[3-6]

The mechanism for the heterogeneous formation of NPAHs has been explored. The kinetics and products of the heterogeneous reactions of surface-bound PAHs with NO_2,[7, 8] OH radicals,[9-11] N_2O_5,[12] NO_3 radicals,[13, 14] O_3,[15, 16]and NO[9] have been investigated using various substances as atmospheric particle models. Because NO_3 radicals play an important role in atmospheric chemistry under dark conditions, particular attention has been paid to the heterogeneous reactions of particulate PAHs upon exposure to $N_2O_5/NO_3/NO_2$. Zhang et al. reported that mono-nitro-, di-nitro-, and poly-nitro-PAHs and their derivatives are produced in the heterogeneous reactions of suspended PAH particles and NO_3 radicals.[13] Shiraiwa et al. reported that the rate constants for the surface-layer reactions of PAHs with NO_3 radicals are in the range of 10^{-15} and 10^{-12}cm$^2\cdot$s^{-1}.[17] Gross et al. reported that the reactive uptake coefficient of the NO_3 radical on the surface of solid PAHs ranges between 0.059 (+0.11/−0.049) at 273 K and 0.79 (−0.21/−0.67) at room temperature.[18] Liu et al. reported that the effective reaction rates of the heterogeneous reaction between suspended four-ring PAH particles and NO_3 radicals are of the order of 10^{-12}–10^{-11} cm^2 s^{-1}, and the uptake coefficient of the NO_3 radical ranges between 0.06 and 0.57.[14]

Zimmermann et al. suggested that, for PAHs that exist in both the gas and particle phases, the heterogeneous formation of particle-bound NPAHs represents a minor formation route compared to the gas-phase formation; however, their studies could not disprove that the heterogeneous reaction of a NO_3 radical is a more important sink for PAHs than NO_2, HNO_3, or O_3.[19]

Although a mechanism has been recently suggested based on the gas-phase chemistry of PAHs with the NO_3 radical, specific markers for the radical-initiated isomer products (2-nitrofluoranthene and 2-nitropyrene) were not observed during the heterogeneous chemical processes.[18, 20, 21] Ringuet et al. reported the first observation of the heterogeneous formation of 2-nitropyrene from particulate pyrene oxidation in the presence of O_3/NO_2, questioning its use as an indicator of NPAH formation in the gaseous phase.[22] Thus, the reaction mechanism of heterogeneous nitration has not been unequivocally identified.

Recent studies have suggested that high concentrations of N_2O_5 and NO_2, either in experiments or the real atmosphere, may prevent the NO_3 radical from being accommodated on particle surfaces and reacting; this may suppressNO_3 radical-initiated heterogeneous reactions.[18, 19, 21] To explore whether this problem of blocking reaction sites has a significant impact on the heterogeneous reactions that occur on the PAH particle surface, we conducted an in-depth investigation of the heterogeneous oxidation of suspended pyrene (PY) particles by $N_2O_5/NO_3/NO_2$ in the presence of O_3. Contrasting order-of-exposure experiments between PY and N_2O_5—O_3 and O_3—N_2O_5, and a series of heterogeneous reactions of suspended PY particles by exposure to N_2O_5 (~8 ppm) in the presence of O_3 (at concentrations ranging from ~2.5 to ~30 ppm) were conducted.

Experimental section

Experimental setup

All experiments were conducted in the dark at room temperature (298 ± 3 K) and atmospheric pressure (~96 kPa). The relative humidity in the chamber ranged between 40% and 50%. The schematic diagram of the experimental setup, shown in Figure 1, was described in previous studies.[14]

The experimental setup consists mainly of a 120-L aerosol reaction chamber,[23] online and offline analytical instruments, an aerosol generator, an ozone generator, and a N_2O_5-vapor manipulator. The online and offline analytical instruments include a laboratory-built vacuum ultraviolet photoionization aerosol time-of-flight mass spectrometer (VUV-ATOFMS), a scanning mobility particle size (SMPS), an ozone monitor (Model 202, 2B Technologies Corp), and a gas chromatograph/mass spectrometer (GC-MS). The VUV-ATOFMS was used to online-monitor the PAH particles and their reaction products in the reaction chamber. A detailed description of the VUV-ATOFMS has been presented elsewhere.[24] The SMPS, consisting of a differential mobility analyzer (DMA, TSI 3081) and a condensation particle counter (CPC, TSI 3010), was employed to measure online the size distribution and mass concentration of the PY particles. The measured mean diameters and mass concentration of PY particles were 367 ± 20 nm and 244 μg m^{-3}, respectively; the geometric standard deviation of the particles was 1.2. The particle surface-to-volume ratio was ~6.43 × 10^9 nm^2 cm^{-3} in the experiments. The partitioning ratio of PY was estimated to be 4.3 ×10^{-4} cm^3 μg^{-1} under our experimental conditions (seeing SI). The GC-MS consisted of an HP model series 6890 gas chromatograph coupled with an HP model 5973 mass-selective detector with a 70-eV electron impact ionizer (Agilent Technologies, Massy, France); this was used offline to identify the nitropyrene isomers (NPY).

N_2O_5/NO_3/NO_2 preparation and aerosol generator

106 The procedures for producing the aerosol particles and N_2O_5 were similar to those
107 recently reported.[14, 25, 26] NO_3 radicals and NO_2 were generated from the thermal
108 decomposition of N_2O_5 at room temperature (eq. R_1). N_2O_5 was synthesized by
109 dehydrating concentrated nitric acid. Fuming nitric acid (~20 mL) was introduced into
110 a glass bottle placed in a 223 K cooling bath. Then, P_2O_5 powder was gradually added
111 into the nitric acid and thoroughly mixed until the slurry was too thick to stir. In
112 preparation of N_2O_5 , a ~25 mm thick layer of P_2O_5 powder was placed over the slurry
113 (the mixture of P_2O_5 and fuming nitric acid) to eliminate nitric acid moisture. Next,
114 the bottle was heated in a 313 K water bath. The gaseous N_2O_5 from the slurry was
115 extracted by a pump and collected in a 1 L flask in a liquid nitrogen-cooled Dewar.
116 The synthesized N_2O_5 powder collected in the liquid nitrogen trap appeared as pure
117 white crystals. The collected N_2O_5 powder could be further purified by vacuum
118 pumping at 263 K to remove minor amounts of NO_2. A digital refrigerated circulator
119 bath (233−373 K, DCW-4006, China) was used to maintain a constant temperature in
120 the cooling bath. A glass trap containing N_2O_5 powder was placed in the cooling bath.
121 Since our laboratory lacks the corresponding detecting instruments, N_2O_5 cannot be
122 measured in an independent way. The concentration of N_2O_5 was controlled by
123 changing its vapor pressure by adjusting the temperature of the bath. O_3 was prepared
124 by passing O_2 through a commercial ozonizer (NBF30/W); its initial concentration in
125 the mixture was measured with an ozone monitor.

126 $$N_2O_5(g) \rightleftharpoons NO_2(g) + NO_3(g) \qquad (R_1)$$

127 An electric tube furnace, equipped with two tandem quartz tubes [50 cm (length) × 3
128 cm (inner diameter)] wrapped in heating tape so as to create a linear hot-to-cool
129 temperature gradient, was used to produce the PY aerosol. Because of the complexity
130 of natural particles, azelaic acid was used to produce nuclei in this study. It has the
131 advantage of having limited reactivity toward gas-phase oxidants and can form a
132 stabilized aerosol distribution.[27] Azelaic acid was placed in the first tube (463 ± 1 K),

and the PY sample in the second tube (453 ± 1 K). A volumetric flow of 0.6 L min^{-1} of N_2 controlled by a mass flow controller (MFC, D08-2F) was used to send the mixed aerosols coated with PY into the reaction chamber through the electric tube furnace.

Product collection and analysis

After exposure to $N_2O_5/NO_3/NO_2/O_3$ in the reaction chamber, the suspended particles in ~75% of the chamber volume were collected with a pre-cleaned glass microfiber filter (GMF, 25 mm diameter, 0.7 μm pore size, Whatman). A schematic diagram of the collection procedure is shown in Figure S1. The filter was connected to a sample pumping (ACO-016, 450 L/min). The collected PY was extracted with ~10 ml dichloromethane. The extraction was carried out for 1 min in a KH-5200B sonicator (Kunshan Hechuang Sonicator Co. Ltd), and concentrated to a volume of ~2 ml by evaporation under a gentle stream of high purity nitrogen, and then analyzed offline using GC-MS. The relative yields of formed NPY isomers under different experimental conditions were compared through the relative abundances of NPY from the results of GC/MS analyses.

The National Institute of Standards and Technology (NIST) Mass Spectral Library 2005 was employed to identify the reaction products. An aliquot of the samples (5 μL) was introduced into the GC-MS system in the pulsed splitless mode. The column used for the analyses was a 30 m × 0.25 mm i.d. × 0.25 μm film thickness DM-1701ms (Agilent Technologies). The temperature of the vaporizer was kept at 270 °C. The initial oven temperature was set to 40 °C for 2 min; it was then increased step-by-step to 150 °C (by 20 °C min^{-1}), 220 °C (by 10 °C min^{-1}), and 270 °C (by 5 °C min^{-1}); the temperature was kept for 10 min at each of the 3 levels. Helium was used as the carrier gas at a constant flow rate of 1 mL min^{-1}. The interface temperature was kept at 270 °C throughout the GC-MS assay. A mass range between *m*/*z* 50 and

500 was used for quantitative determinations. The GC-MS data were obtained via GC-MS selected ion monitoring (SIM) of the molecular ion (*m/z* 247).

Chemicals

PY (98%, Sigma Aldrich), azelaic acid (98%, Sigma Aldrich), dichloromethane (chromatographic grade, Sinopharm Chemical Reagent Beijing Co., Ltd.), and absolute ethyl alcohol (≥ 99.7%, Sinopharm) were used in the experiments.

Exposure experiments

Wall loss

Both NO_3 radicals and N_2O_5, as two major oxidants in our study, could not been online monitored due to the limitation of our current experimental condition. Thus, the wall loss characterized for NO_3 radical and N_2O_5 could not been characterized. As for the wall loss of O_3 and NO_2, 30 ppm O_3 and 10 ppm NO_2 are separately introduced into the chamber. The results show that their concentrations are basically constant after their concentrations stabilization. Thereby, the wall loss of O_3 and NO_2 in the chamber could be negligible.

The wall loss of PY particles monitored with the VUV-ATOFMS in the absence of oxidants are below 5% for 500 s, thus, the wall loss of PY particles have not apparent impact to their heterogeneous degradation.

Contrast experiments

To establish whether the phenomenon of blocking reaction sites has a significant impact on heterogeneous reaction mechanisms of particulate PY and $N_2O_5/NO_3/NO_2$, two different types of experiments were carried out. In the $N_2O_5-O_3$ exposure, the

PY aerosol in the chamber was first exposed to ~1.5 ppm N_2O_5 for ~3 min, followed by a heterogeneous exposure for 3 min to O_3 (after ~5.5 ppm O_3 was introduced into the chamber). The sequence of introducing O_3 and N_2O_5 into the chamber in the O_3—N_2O_5 exposure was simply reversed from that of the N_2O_5—O_3 exposure. We assumed that the effect of blocked reaction sites on the heterogeneous nitration mechanism would be negligible, and the observed 2-NPY would be mainly formed in the gas-phase reaction following deposition onto the particles. Based on this hypothesis and considering the same mass concentration of PY aerosol, because N_2O_5 was first introduced in the chamber and can produce the NO_3 radical (R_1), the NO_3 radical-initiated NPY yield in the N_2O_5—O_3 exposure (especially for 2-NPY formed in the gas-phase reaction) should be higher than that in the O_3—N_2O_5 exposure due to the longer exposure time in the chamber.

Effect of different O_3concentrations

To further clarify whether the high concentrations of N_2O_5 and NO_2 used may block the NO_3 radical from being accommodated on the surface and reacting, a series of heterogeneous reactions of suspended PY particles with N_2O_5 (~8 ppm) in the presence of different O_3 concentrations (ranging between ~2.5 ppm and ~30 ppm) was conducted. The concentrations of O_3 and N_2O_5 in this work are higher than those found in the atmosphere. To investigate whether adsorbed molecules would prevent other reactants from accessing reactive substrate species under real atmospheric conditions, heterogeneous exposures of PY particles to N_2O_5 (~500 ppb) in the presence of O_3 (~150 ppb) were also carried out. However, the results showed that no 2-NPY was formed after exposure for 20 min. Since PY particles in the chamber were continuously sedimented as the reaction time was prolonged (>20 min), experiments at lower concentration with much longer reaction times could not be carried out in our reaction chamber. Additionally, to the best of our knowledge, several previous and recent studies have shown that both the effective reaction rate constants of PAHs with NO_3 radicals and the reactive uptake coefficient of the NO_3 radical on the surface of

the particulate or adsorbed PY are 5–7 orders of magnitude faster than those of adsorbed PAHs oxidized by O_3, NO_2, and N_2O_5.[7, 14, 16, 18, 28] Thus, it can be concluded that 2-NPY might be formed via the heterogeneous reaction of the NO_3 radical and PY in the real atmosphere if the reaction time is long enough.

Results and discussion

Contrast experiments

Figures 2A-B show the NPY distributions obtained from the two exposure orders. Similar to the results described by Ringuet et al.,[29] the NO_3 radical-initiated NPY isomers (2-NPY and 4-NPY) are clearly observed. However, contrary to our hypothesis, the amounts of 2-NPY and 4-NPY are significantly enhanced in the O_3—N_2O_5 exposure. Previous studies showed that 2-NP was only formed via the gas-phase reaction of PY and the NO_3 radical in the presence of higher NO_2 concentrations in the gaseous phase.[30] Additionally, Zimmermann et al. concluded that 1-NPY is unlikely to be formed by NO_3 radical-initiation, but rather, by nitration that occurs after the adsorption of N_2O_5. Therefore, the traditional use of 2-NP as a marker of NPAH formation in the gaseous phase seems questionable.[31, 32] Our experimental results reveal that the observed 2-NPY arises mainly from the heterogeneous reaction; the contribution of gas-phase 2-NPY is negligible in the experiments. The ratio of the NO_3 radical-initiated isomers (2-NPY and 4-NPY) to 1-NPY increases from ~37.8% in the N_2O_5—O_3 exposure to ~ 80.1% in the second experiment. Given that O_3 is first introduced into the chamber, a mixture of PY particles and O_3 should be obtained within 3 min, and more reaction sites on the PY particle surfaces should be surrounded by O_3 in the O_3—N_2O_5 exposure. We thus concluded that more reactive NO_3 radicals may be formed on the particle surface via the surface reaction R_2, and

the NO_3 radical-initiated heterogeneous reaction should be promoted on the particle surface.[33]

$$NO_2 + O_3 \rightarrow NO_3 \quad (R_2)$$

However, a rather different scenario should take place in the $N_2O_5-O_3$ exposure, i.e., the NO_3 radical-initiated reaction mechanism may be suppressed to some extent because the large concentrations of N_2O_5 and NO_2introduced at first may interfere with the heterogeneous reaction between the NO_3 radical and PY by blocking NO_3 radicals from being accommodated on the surfaces and reacting. Additionally, we noted that the amount of the 1-NPY isomer observed in the $O_3-N_2O_5$ exposure is significantly higher than that in the $N_2O_5-O_3$ exposure. We speculate that the higher NO_3 concentration in the $O_3-N_2O_5$ exposure and the larger NO_3 uptake coefficients on the PY particle surface (approximately 4–5 orders of magnitude higher than those of N_2O_5) cause a larger production of N_2O_5 on the surface of the PY particles;[18] to some extent, this indirectly promotes the N_2O_5-initiated ionic electrophilic nitration mechanism. However, additional studies are needed to clarify whether the NO_3 radicals and NO_2 can form N_2O_5 near the PY surface. Based on our experimental results, a higher N_2O_5 concentration (in the real atmosphere and in the absence of O_3) can inhibit NO_3 radical-initiated heterogeneous reactions. In contrast, the higher NO_3 concentration can promoteN_2O_5-initiated electrophilic nitration. Thereby, we conclude that the two reaction mechanisms should be competitive and mutually reinforce each other to some extent. The operative reaction mechanisms are highly dependent on the concentrations of the nitric oxides (N_2O_5 and NO_3 radicals) on the surface of atmosphere particles. High concentrations of N_2O_5 and NO_2 under either experimental or real atmospheric conditions can prevent NO_3 radicals from being accommodated on the surfaces and reacting, thereby suppressing the formation of the NO_3 radical-initiated isomers.

Effect of different O_3concentrations

Increasing NO_3 radical concentrations and decreasing NO_2 concentrations were observed with increasing O_3 concentrations (Table 1). In all different O_3 concentration exposures, the heterogeneous reaction time and the mixing times between the PY particles and oxidants (O_3 and the NO_x species) were consistent (~8 min). Figures 3A–E show the NPY isomers distribution obtained from these exposures. The experimental results from Ringuet et al. reported that formation of 2-NPY by the heterogeneous reaction of PY with O_3/NO_2 was clearly observed.[29] However, this is not consistent with the results obtained in the real atmosphere, since no 2-NPY is formed in the atmospheric heterogeneous reaction of $N_2O_5/NO_3/NO_2/O_3$ due to a lower NO_3 concentration. This may result from the lower NO_3/N_2O_5 ratio at 298 K in the real atmosphere compared to that used in this study. The NO_3/N_2O_5 ratio at 298 K in the real atmosphere was estimated to be ~0.006 using the following equation:

$$\frac{[NO_3]}{[N_2O_5]} = 1/\{K_{eq}[NO_2]\} = 1/\{3 \times 10^{-27}\, exp(10990/T)\, [NO_2]\} \quad (1)$$

where $[NO_2]$ is the NO_2 concentration in the real atmosphere (up to ~200 ppb in polluted air),[34-38] and K_{eq} represents the equilibrium constant for $N_2O_5(g) \rightleftarrows NO_2(g) + NO_3(g)$. In the present study, the $[NO_3]/[N_2O_5]$ ratios (ranging between 0.018 and 0.61, Table 1) in the chamber experiments are significantly larger than those in the ambient atmosphere. It should be noted that a remarkable increase in the 2-NPY yield is observed as the initial concentration of O_3 is gradually increased (Figures 3A-D), which further questions its use as an indicator of NPAH formation in the gaseous phase. This may be caused by the formation of more reactive NO_3 radicals, or a gradual increase in the $[NO_3]/[N_2O_5]$ ratios, which occurs when the O_3 concentration is increased in the chamber (Table 1). In this case, the NO_3-initiated reaction mechanism may be favored in the heterogeneous reaction process over the N_2O_5-initiated ionic electrophilic nitration mechanism, since the equilibrium concentration of N_2O_5 is constant under different O_3 concentrations. We

thus conclude that the blocking mechanism occurring on the particle surface in the heterogeneous process should be gradual. Similar to the observations of the discussed contrast experiments (Figure 2), the 1-NPY isomer yield (Figure 3A-C) also increased with the initial concentration of O_3 (from 2.5 to 13.5 ppm). This confirms that the N_2O_5-initiated ionic electrophilic nitration mechanism may be reinforced to some extent due to the higher uptake coefficient on the particle surface and the higher gas-phase concentration of NO_3 radicals. Surprisingly, the yields of 2-NPY and 1-NPY (Figure 3E) in the presence of ~30 ppm O_3 are significantly smaller than those shown in Figures 3B-D. This may result from the increase in O_3 concentration and the decrease in NO_2 concentration that occur under equilibrium conditions. We suggest three possible explanations for this phenomenon. First, it should be noted that the NO_2 concentration is clearly lower than that of the NO_3 radical under equilibrium conditions when ~30 ppm O_3 is added into the chamber (Table 1). The NO_3 radical-initiated mechanism requires both NO_3 and NO_2 to proceed (i.e., the NO_3 initiates the reaction and NO_2 is required at a later step to form the final product). Atkinson et al. also suggested that the gas-phase formation of 2-NPY in the $N_2O_5/NO_3/NO_2$ exposure is a function of the NO_2 concentration (with an excess of NO_2).[4] Thereby, the lower NO_2 concentration in the chamber may suppress the corresponding NO_3-initiated reaction mechanism. Similarly, we concluded that this may also occur for the heterogeneous formation of 2-NPY. Second, the TOF mass spectra of some ozonation products of PY located at *m/z*= 205, 218, and 250 are clearly observed, because the heterogeneous reaction between particulate PY and O_3 may dominate when an excess of O_3 (~30 ppm) is employed (Figure 4).[39] Finally, although our previous study suggests that only trace amounts of pyrenequinone (*m/z* 232) are produced during the O_3-only exposure (~30 ppm),[39] according to this work, significant amounts of pyrenequinone and mono-nitropyrenequinone (*m/z* 277), as well as 2-NPY (Figure 3), are the main NO_3 radical-initiated products due to the occurrence of NO_3 radicals in the presence of ~30 ppm O_3. The

317 mono-nitropyrenequinone is believed to form from further reaction of the
318 pyrenequinone with NO_3 radicals.

319 Additionally, it has been recognized that O_3 and NO_x (NO_3 radicals, NO_2, and
320 N_2O_5) are ubiquitous and coexistent in the atmosphere. However, most chamber
321 studies of NO_3-derived nitro-PAHs generate NO_3 through the thermal dissociation of
322 N_2O_5 in order to minimize the complexity caused by introducing a second oxidant.[13,
323 18, 40, 41] Fewer studies have been done using the atmospherically more relevant
324 conditions of introducing both NO_x and O_3 into the chamber to mimic this full range
325 of nighttime oxidation chemistry.[22] Thereby, the results obtained also highlight the
326 dependence of the heterogeneous formation of NPAHs on the complicated nature of
327 atmospheric oxidants.

328

329 ## Conclusions

330 This study clearly showed that the N_2O_5-initiated ionic electrophilic nitration
331 mechanism and the NO_3 radical-initiated mechanism may both be operative in
332 atmospheric heterogeneous processes. However, since the concentrations of N_2O_5 (up
333 to ~10 ppb), O_3 (80~150 ppb), and NO_2 (up to ~200 ppb) in the real atmosphere are
334 significantly higher than the concentration of NO_3 radicals (which ranges between <
335 10 and 430 ppt),[34-38] these oxidants may block NO_3 radicals from being
336 accommodated on the surfaces and reacting. Thus, NO_3 radical-initiated
337 heterogeneous reactions may be suppressed on the particle surface. The phenomenon
338 of blocking reaction sites may be ubiquitous on the surfaces of atmospheric aerosol
339 particles and have a significant impact on the heterogeneous nitration mechanism.

However, the extent to which this affects the heterogeneous reactions of PY and $N_2O_5/NO_3/NO_2$ in the real atmosphere due to the lower NO_x concentrations will need further investigation. Additionally, this explains why 2-NPY, an indicator for the NO_3 radical-initiated reactions of the parent PAHs, was not observed in the heterogeneous processes investigated in previous studies; our findings provide supplementary knowledge for the heterogeneous reaction mechanism. Furthermore, the blocked-sites phenomenon occurring in the heterogeneous reaction was only investigated in this study from a macroscopic perspective. To further explore the blocked-sites phenomenon in atmospheric heterogeneous processes, computer simulations and experiments, especially with respect to the surface coverage of competing reactants on particle surfaces, are needed.

Supporting Information.

Experimental section.

Estimation of oxidants concentrations in the new equilibrium system.

Acknowledgement

This work was supported by the National Natural Science Foundation of China (Grant Nos. 21277155 and 21207143) and the Creative Research Groups of China (No. 51221892).

References

1. K. Ravindra, R. Sokhi and R. Van Grieken, *Atmos. Environ.*, 2008, **42**, 2895-2921.

2. I. W. G. o. t. E. o. C. R. t. Humans, *International Agency for Research on Cancer.* 2010, **92**, 1.

3. J. Sasaki, S. M. Aschmann, E. S. Kwok, R. Atkinson and J. Arey, *Environ. Sci. Technol.*, 1997, **31**, 3173-3179.

4. R. Atkinson, J. Arey, B. Zielinska and S. M. Aschmann, *J. Phys. Chem. Kinet.*, 1990, **22**, 999-1014.

5. J. Arey, B. Zielinska, R. Atkinson, A. M. Winer, T. Ramdahl and J. N. Pitts Jr, *Atmos. Environ (1967).,* 1986, **20**, 2339-2345.

6. R. Atkinson, J. Arey, B. Zielinska and S. M. Aschmann, *Environ. Sci. Technol.*, 1987, **21**, 1014-1022.

7. M. L. Nguyen, Y. Bedjanian and A. Guilloteau, *J. Phys. Chem.*, 2009, **62**, 139-150.

8. J. Ma, Y. Liu and H. He, *Atmos. Environ.*, 2011, **45**, 917-924.

9. W. Esteve, H. Budzinski and E. Villenave, *Atmos. Environ.*, 2004, **38**, 6063-6072.

10. W. Esteve, H. Budzinski and E. Villenave, *Atmos. Environ.*, 2006, **40**, 201-211.

11. K. Miet, H. Budzinski and E. Villenave, *Polycycl. Aromat. Comp.,* 2009, **29**, 267-281.

12. R. M. Kamens, J. Guo, Z. Guo and S. R. McDow, *Atmos. Environ Part A. General Topics.*, 1990, **24**, 1161-1173.

13. Y. Zhang, B. Yang, J. Gan, C. Liu, X. Shu and J. Shu, *Atmos. Environ.*, 2011, **45**, 2515-2521.

14. C. Liu, P. Zhang, B. Yang, Y. Wang and J. Shu, *Environ. Sci. Technol.*, 2012, **46**, 7575-7580.

15. E. Perraudin, H. Budzinski and E. Villenave, *J. Phys. Chem.*, 2007, **56**, 57-82.

16. K. Miet, K. Le Menach, P. Flaud, H. Budzinski and E. Villenave, *Atmos. Environ.*, 2009, **43**, 3699-3707.

17. M. Shiraiwa, R. M. Garland and U. Pöschl, *Atmos. Chem. Phys.*, 2009, **9**, 9571-9586.

18. S. Gross and A. K. Bertram, *J. Phys. Chem. A.*, 2008, **112**, 3104-3113.

19. K. Zimmermann, N. Jariyasopit, S. L. Massey Simonich, S. Tao, R. Atkinson and J. Arey, *Environ. Sci. Technol.*, 2013, **47**, 8434-8442.

20. N. O. A. Kwamena and J. P. D. Abbatt, *Atmos. Environ.*, 2008, **42**, 8309-8314.

21. J. Mak, S. Gross and A. K. Bertram, *Geophys. Res. Lett.*, 2007, **34**, L10804.

22. J. Ringuet, A. Albinet, E. Leoz-Garziandia, H. Budzinski and E. Villenave, *Atmos. Environ.*, 2012, **61**, 15-22.

23. B. Yang, J. Meng, Y. Zhang, C. Liu, J. Gan and J. Shu, *Atmos. Environ.*, 2011, **45**, 2074-2079.

24. J. Shu, S. Gao and Y. Li, *Aerosol. Sci. and Tech.,* 2008, **42**, 110-113.

25. C. Liu, J. Gan, Y. Zhang, M. Liang, X. Shu, J. Shu and B. Yang, *J. Phys. Chem. A.*, 2011, **115**, 10744-10748.

26. P. Zhang, Y. Wang, B. Yang, C. Liu and J. Shu, *Chemosphere.* 2014, **99**, 34-40.

27. P. Zhang, W. Sun, N. Li, Y. Wang, J. Shu, B. Yang and L. Dong, *Environ. Sci. Technol.*, 2014, **48**, 13130-13137.

28. R. M. Kamens, J. Guo, Z. Guo and S. R. McDow, *Atmos. Environ Part A. General Topics.*, 1990, **24**, 1161-1173.

29. J. Ringuet, A. Albinet, E. Leoz-Garziandia, H. Budzinski and E. Villenave, *Atmos. Environ.*, 2012.

30. J. N. Pitts Jr, J. A. Sweetman, B. Zielinska, A. M. Winer and R. Atkinson, *Atmos. Environ (1967).*, 1985, **19**, 1601-1608.

31. A. Albinet, E. Leoz-Garziandia, H. Budzinski and E. Villenave, *Sci. Total. Environ.*, 2007, **384**, 280-292.

32. A. Albinet, E. Leoz-Garziandia, H. Budzinski, E. Villenave and J.-L. Jaffrezo, *Atmos. Environ.*, 2008, **42**, 43-54.

33. U. Pöschl, Y. Rudich and M. Ammann, *Atmos. Chem. Phys.*, 2007, **7**, 5989-6023.

34. M. Aldener, S. S. Brown, H. Stark, E. J. Williams, B. M. Lerner, W. C. Kuster, P. D. Goldan, P. K. Quinn, T. S. Bates and F. C. Fehsenfeld, *J. Geophys. Res.* : *Atmos (1984–2012)* ., 2006, **111**.

35. U. Platt, D. Perner, A. M. Winer, G. W. Harris and J. N. Pitts, *Geophys. Res. Lett.*, 1980, **7**, 89-92.

36. J. Stutz, B. Alicke, R. Ackermann, A. Geyer, A. White and E. Williams, *J. Geophys. Res.*, 2004, **109**, D12306.

37. S. Brown, *Science.*, 2006, **1120120**, 311.

38. D. A. Knopf, S. M. Forrester and J. H. Slade, *Phys. Chem. Chem. Phys.*, 2011, **13**, 21050-21062.

39. S. Gao, Y. Zhang, J. Meng and J. Shu, *Atmos. Environ.*, 2009, **43**, 3319-3325.

40. Y. Zhang, B. Yang, J. Meng, S. Gao, X. Dong and J. Shu, *Atmos. Environ.*, 2010, **44**, 697-702.

41. N. Jariyasopit, M. McIntosh, K. Zimmermann, J. Arey, R. Atkinson, P. H.-Y. Cheong, R. G. Carter, T.-W. Yu, R. H. Dashwood and S. L. Massey Simonich, *Environ. Sci. Technol.*, 2013, **48**, 412-419.

Figure Caption

Fig. 1. The schematic diagram of the experimental setup.

Fig. 2. The NPY isomer distributions observed in the N_2O_5—O_3 (A) and the O_3—N_2O_5 exposure (B).

Fig. 3. The NPY isomer distributions observed during the $N_2O_5/NO_3/NO_2$ exposure in the presence of different initial O_3 concentration ranging from 2.5 ppm to 30 ppm.

Fig. 4. TOF mass spectra of reaction products during the $N_2O_5/NO_3/NO_2/O_3$ exposure: ~20 ppm O_3 (black line) and ~30 ppm O_3 (red line).

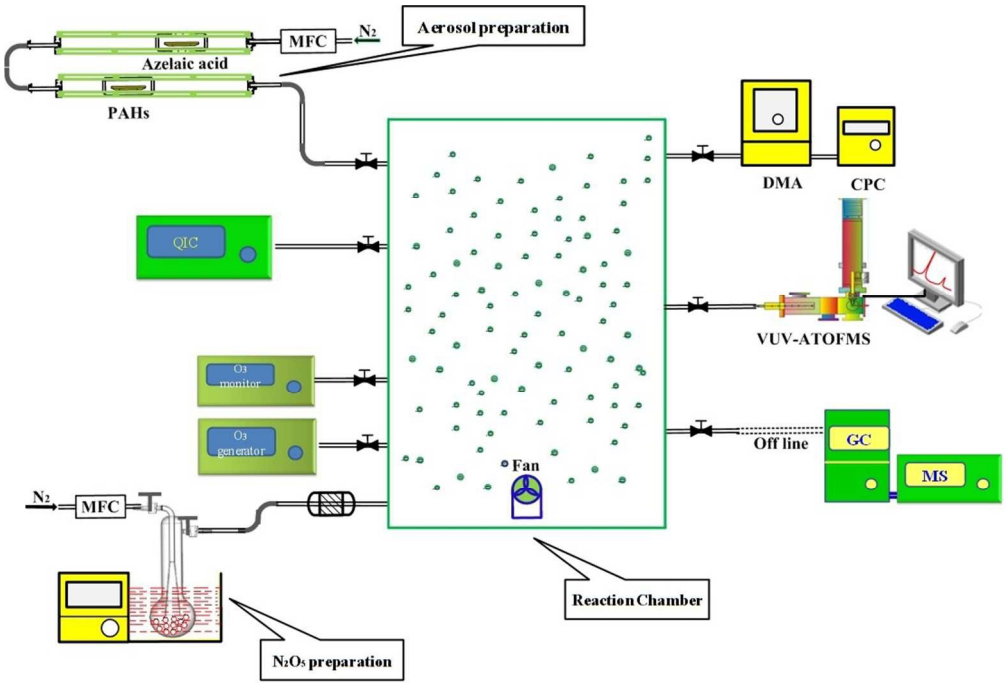

292x198mm (96 x 96 DPI)

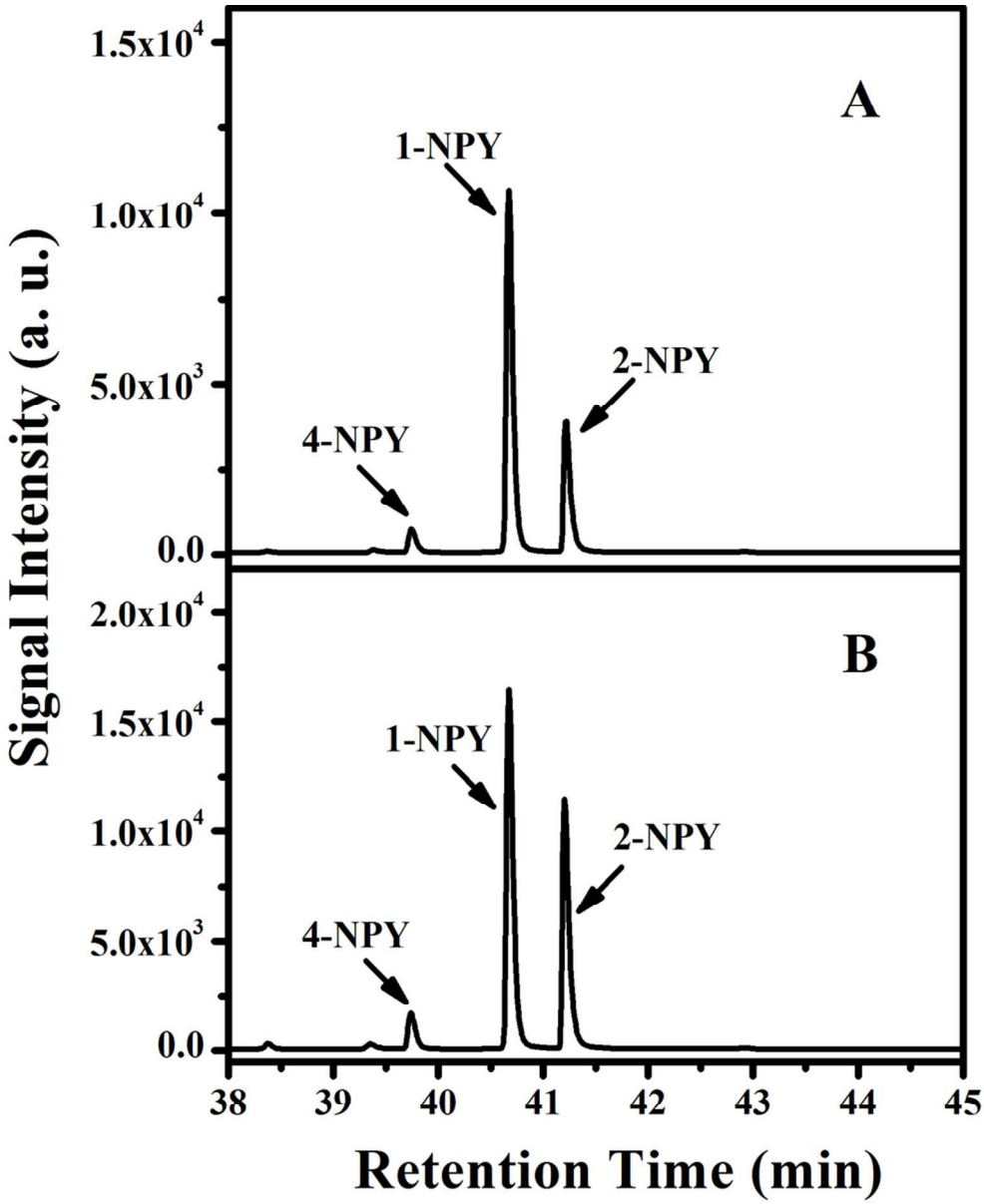

90x109mm (300 x 300 DPI)

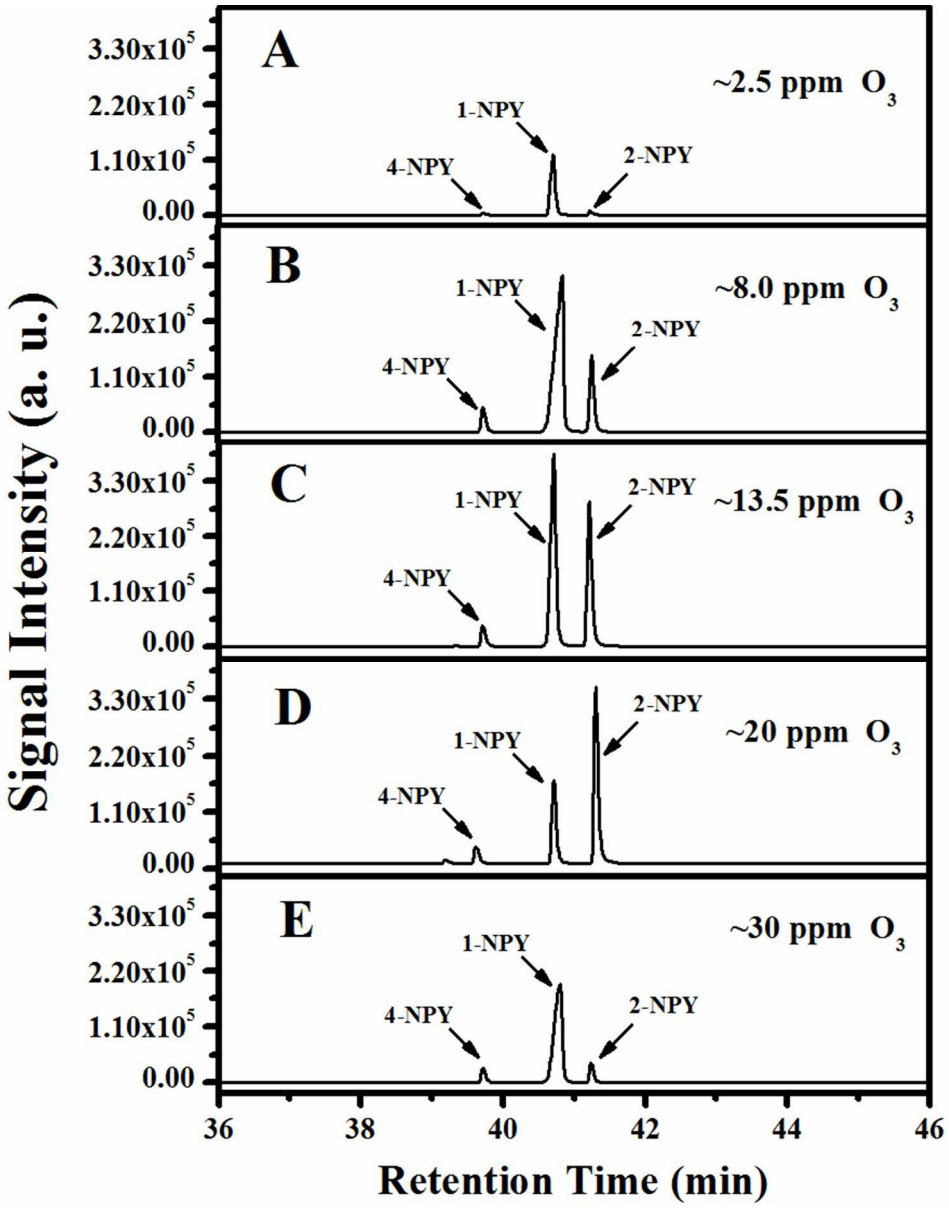

74x94mm (300 x 300 DPI)

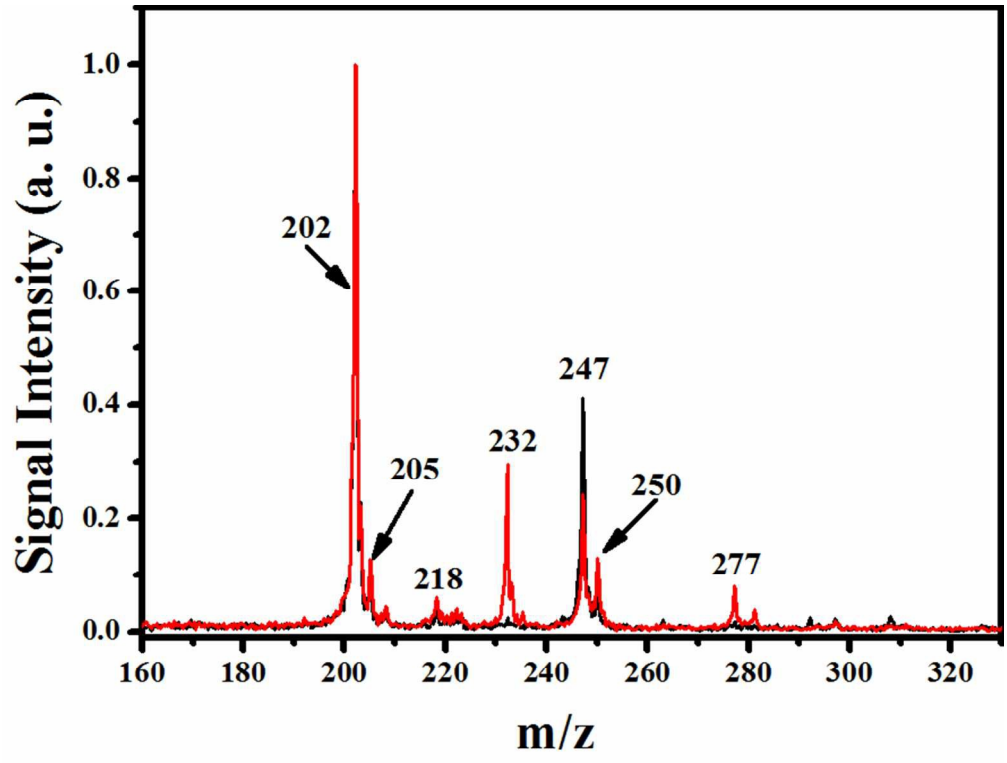

74x56mm (300 x 300 DPI)

Table 1. The concentrations of NO_2, N_2O_5, O_3 and NO_3 radicals and the $[NO_3]/[N_2O_5]$ ratio in different experiments

Exposures	Initial Conc (molecules cm^{-3})		Equilibrium Conc (molecules cm^{-3})				
	N_2O_5	O_3	N_2O_5	NO_2	NO_3	O_3	NO_3/N_2O_5
Contrast Exposures	6.15×10^{13}	6.2×10^{13}	6.00×10^{13}	4.54×10^{11}	4.23×10^{11}	6.11×10^{11}	0.07
		5.6×10^{14}		1.82×10^{12}	1.67×10^{11}	5.90×10^{13}	0.018
		2.0×10^{14}		1.02×10^{12}	2.99×10^{12}	1.94×10^{14}	0.032
Effect	2.00×10^{14}	3.30×10^{14}	9.50×10^{13}	7.82×10^{11}	3.89×10^{12}	3.28×10^{14}	0.041
		4.90×10^{14}		6.43×10^{11}	4.74×10^{12}	4.87×10^{14}	0.05
		7.40×10^{14}		5.25×10^{11}	5.81×10^{12}	7.32×10^{14}	0.061

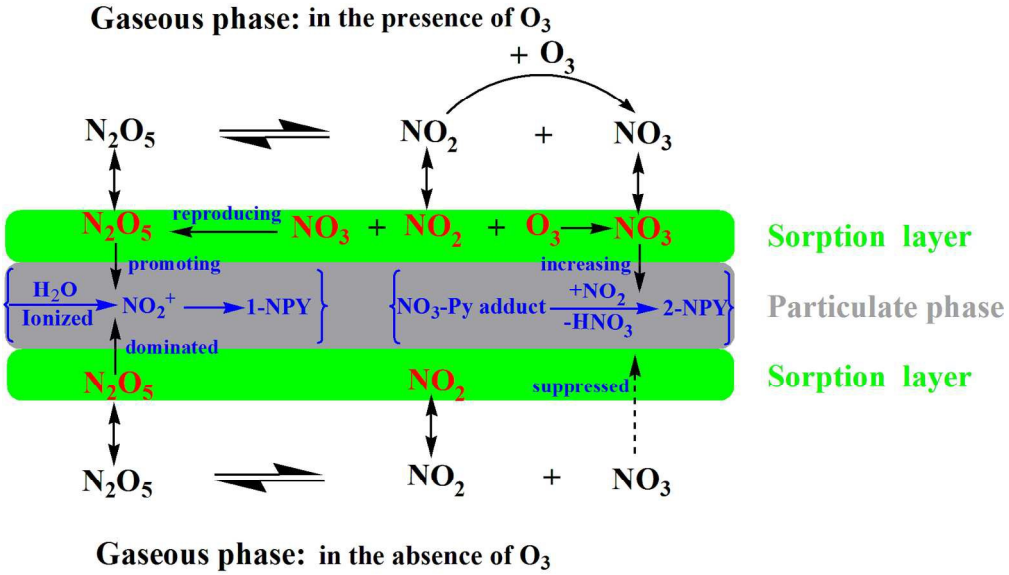

154x88mm (300 x 300 DPI)